Chapter 11
A Variation on the Expanding Ring Tensile Test

Brady Aydelotte, Warren Jones, Nathan Woods, and Colin Merriman

Abstract The expanding ring tensile test is a method for collecting high strain rate tensile data. It offers high strain rates and large deformations. It can be performed in several ways, including the use of laboratory guns, explosives, and electromagnetic expansion. Each of these methods possess advantages and disadvantages.

In this work we investigate using an RP-4 SC detonator to provide energy for expanding ring experiments and an expanding tube experiment. Three different geometries are considered. We explore the effects of different geometry choices and the ability to extract material model parameters from this version of the expanding ring tensile test.

Keywords Tension, Strength, Expanding Ring, Polymer, Detonator

Introduction

The expanding ring tension test is a method for collecting high strain rate tensile data. It can be performed in a number of different ways including explosives [1], [2], [3], [4], [5], electromagnetic expansion [6], [7], [8], exploding wire [9, pp. 105–106], [10], and a version of it is performed using gun impact on an elastomer filler [11], [12]. Some of the benefits of this approach include allowing the experimentalist to access large plastic strains and high strain rates more easily than most variants of the Kolsky bar tension test.

In this work we examined the possibility of using an RP-4 SC detonator [13] to provide the energy for ring or cylinder expansion. It is somewhat analogous to the method employed by [11], [12] in using a projectile to apply pressure to a filler inside a sample tube to cause expansion and fragmentation. We examined three different candidate designs for coupling the RP-4 SC's energy into a sample using a polymer. Then we examined the viability of these tests for optimization-based fitting of constitutive model parameters by performing a sensitivity analysis.

Method

The ALEGRA hydrocode [14] was used to model the different experimental configurations. An Eulerian, 2D axisymmetric mesh was used for the evaluations. Model response was adequately converged at a cell size of 0.12 mm for the RP-4 SC [15] and this cell size was used for all 2D modeling.

The material models used for this study are shown in Table 1. The constants for the models are drawn from ALEGRA's included constitutive library except where specified.

The RP-4 SC model was taken from [15] which was derived from [16]. The RP-4 SC formation was modeled until the jet tip moved 3 charge diameters from the initial location of the front (open) portion of the copper liner. The model was exported as a collection of exodus files containing complete geometry, thermodynamic and kinetic state of the formed jet. The same formed RP-4 SC model was used for all subsequent candidate design simulations.

The first geometry was a plain cylinder (PC) with a polymer insert and steel caps, shown in Figure 1 (a). This was a control geometry, primarily to determine if the ring expansion geometries offer any meaningful improvement in their ability to fit constitutive model parameters. The second geometry was a ring expansion geometry (R1), shown in Figure 1 (b). This is very similar to the PC except the polymer cylinder was made thin relative to its diameter. The last simulated experimental

Brady Aydelotte · Warren Jones · Nathan Woods · Colin Merriman
Idaho National LaboratoryIdaho Falls, ID 83415
e-mail: brady.aydelotte@inl.gov; warren.jones@inl.gov; charles.woods@inl.gov; colin.merriman@inl.gov

Paul Allison et al. (eds.), *Dynamic Behavior of Materials, Vol. 1*, Conference Proceedings
of the Society for Experimental Mechanics Series, https://doi.org/10.13052/97887-438-0827-5_11

Table 1 Material models and equations of state used for different materials. JC refers to either the Johnson-Cook strength [17] or failure [18] model depending on the column. SGL refers to the Steinberg-Guinan-Lund constitutive model [14], [19], [20]. JWL refers to the Jones-Wilkins-Lee equation of state [21]. LANL refers to Los Alamos National Laboratories. SNL refers to Sandia National Laboratories.

Component	Equation of State	Constitutive Model	Failure Model
Air	LANL Sesame 5030	–	–
Confinement Disk, Steel	SNL Sesame 2150	JC 2IN RHA with A=875e6 Pa	JC Steel
Confinement Disk, Copper	SNL Sesame 3325	JC Copper	JC Copper
Expansion Cylinder, Copper	SNL Sesame 3325	JC Copper	JC Copper
Expansion Cylinder, Al	SNL Sesame 3700	JC 6061-T6 Al	JC 6061-T6 Al
Polymer Insert (HDPE)	LANL Sesame 97182 Reactant LANL Sesame 97183 Product Arrhenius Reactive Burn	–	–
RP-4 SC Explosive	JWL Composition C-4	–	–
RP-4 SC Liner	SNL Sesame 3325	SGL Copper	Void insertion P<-2.3 GPa
RP-4 SC Outer shell	SNL Sesame 3700	JC 6061-T6 Al	JC 6061-T6 Al
Sample Ring	SNL Sesame 3700	JC 6061-T6 Al	JC 6061-T6 Al
Sensitivity Analysis model	SNL Sesame 3700	JC 6061-T6 Al with A, B, and N as variables	JC 6061-T6 Al
Tamper, Steel	SNL Sesame 2150	JC 2IN RHA with AJ0=875e6 Pa	JC Steel

geometry, a ring expansion geometry, (R2) had a more sophisticated design for the outer cylinder to give the ring a more uniform push.

DAKOTA [22] was used to perform parametric studies to select the final geometries for the different experimental configurations. These will not be addressed in detail; the final dimensions are shown in Figure 1. Once the geometry was fixed, a sensitivity analysis was performed on each geometry. A random sampling approach was generated using a Latin Hypercube Sampling approach. DAKOTA was allowed to select values of the Johnson-Cook strength model parameters A, B, and n (see Equation 1) and the ring or tube velocity history was modeled. The ring velocity was sampled at five different equally spaced times between the initial rise above zero velocity and the first time its velocity again becomes zero. The Spearman rank correlation sensitivity indices were computed [22].

$$\sigma_Y = \left[A + B(\varepsilon^p)^n\right]\left[1 + Cln\left(\varepsilon^*\right)\right]\left[1 - \theta^M\right] \tag{1}$$

Results

The PC geometry is very simple. The parts are amenable to conventional or additive manufacturing. The radial expansion velocity can be controlled by the thickness of the tube, the diameter of the tube, and the thickness of the confinement disks. The radial and axial velocity of the design shown in Figure 1 a, with a 12 mm inner diameter tube with a 1 mm wall thickness, is shown in Figure 2. The maximum radial velocity for this configuration was 184.8 m/s and the maximum axial velocity is -66.5 m/s. This design has several distinct axial velocity maxima or minima in the velocity curve prior to 20 microseconds.

The R1 geometry is very similar to the PC except for the plastic cylinder design. Some parametric studies were conducted examining the effects of different ring thickness (assuming a square sample ring cross section) with different polymer cylinder thicknesses. The polymer cylinder thickness was minimized to see if that would reduce the axial velocity component of the ring. A disc slightly thicker than the ring provided more radial velocity for a given ring size. A slightly undersized polymer disc led to a slightly lower velocity. Equal thickness polymer disc and sample ring yielded adequate velocity. The thicker the ring, the slower for a fixed diameter. Parametric studies determined that a polymer disk thickness equal to the ring thickness resulted in subjectively good ring velocity with little polymer being expelled around the ring to potentially obscure it.

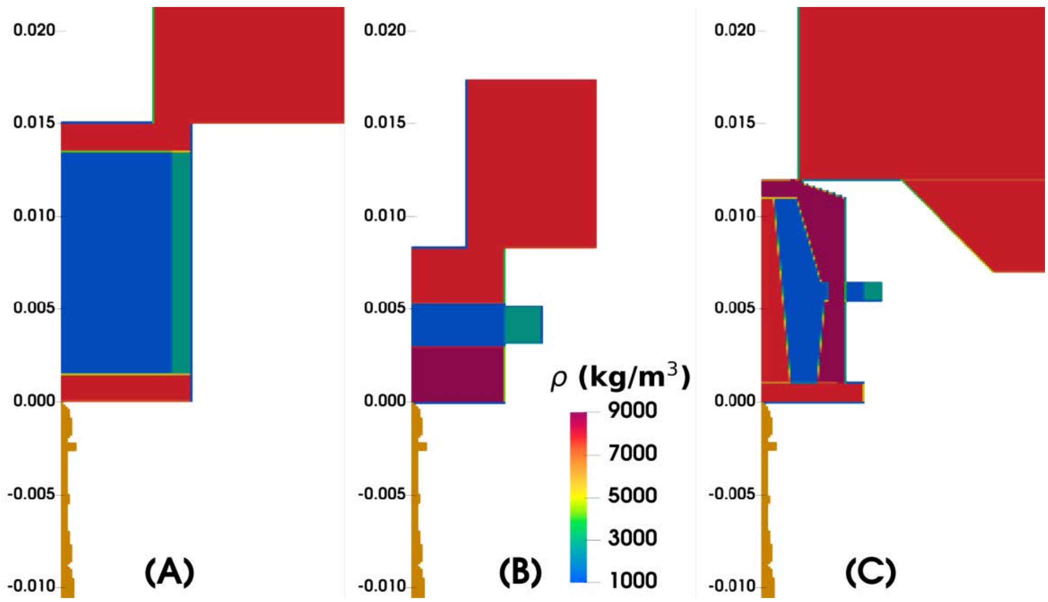

Fig. 1 The three different expansion geometries which were considered; all are radially symmetric about their vertical axes. Dimensions are in meters. Density is plotted for the experimental setups to clarify materials, apart from the shaped charge tip (on the bottom moving up) which is copper colored. The materials used in the design include high density polyethylene, 6061 aluminum, high strength carbon steel, and oxygen free high conductivity copper. (a) The plain cylinder (PC) geometry. (b) The first ring expansion geometry (R1). (c) The second ring expansion geometry (R2).

The radial and axial velocity of the R1 design shown in Figure 1 b, with a 10 mm inner diameter sample ring with a 2 mm wall thickness, is shown in Figure 2. This design exhibits a maximum velocity of 182.5 m/s in this configuration and a maximum axial velocity of -19.7 m/s. The largest axial velocities appear after 20 microseconds.

The R2 ring expansion geometry had a more sophisticated design for the outer cylinder. This design was intended to give the sample ring a more uniform push by shaping the copper buffer, outer tube, and polymer insert. The radial and axial velocity of the R2 design shown in Figure 1 b, with a 11 mm inner diameter sample ring with a 1 mm wall thickness, is

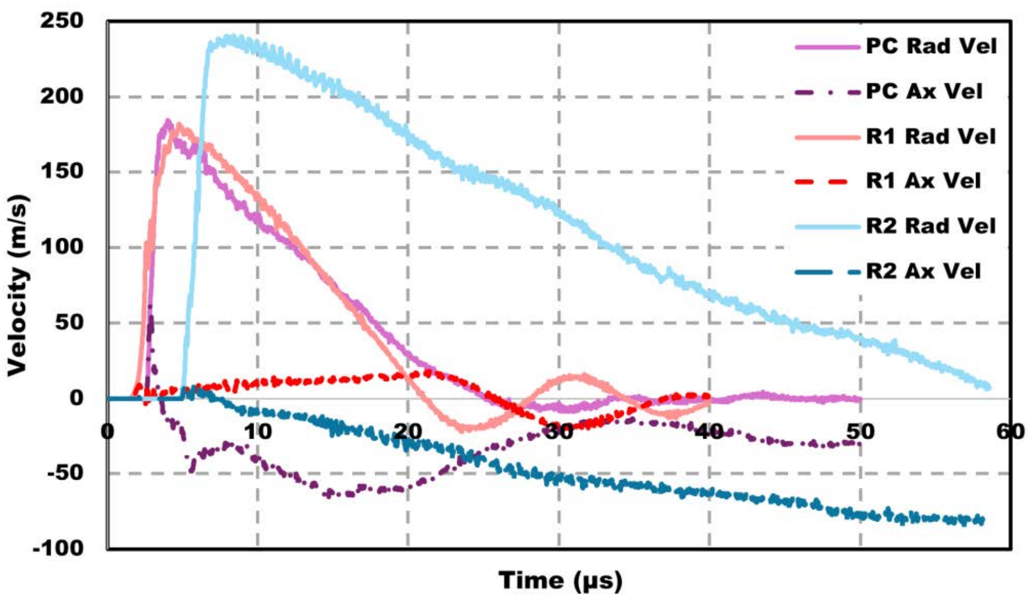

Fig. 2 Plot of radial velocities (the experimental quantity of interest) and the axial velocity (generally undesirable) for the PC, R1, and R2 configurations.

shown in Figure 2. The peak velocity was the highest, of the three designs we considered, at 240.8 m/s with a longer duration of radial velocity greater than zero. The axial velocity was also the highest. However, the maximum occurred at the end of the simulation time window, near 57.5 microseconds.

The sensitivity analysis performed using DAKOTA generated results which are summarized in Figure 3. The absolute value of the sensitivity indices for all the velocity history data points were averaged for Johnson-Cook parameters A, B, and n for each design. The plain cylinder geometry exhibited good sensitivity for A, B, and N, with sensitivity indices which were on average higher than the other two designs. The R2 design averaged the lowest sensitivity indices.

In this case, a good experimental design should exhibit a high degree of sensitivity in the sample velocity to changes in the A, B, and n parameters and all these designs appear to exhibit reasonable sensitivity to the Johnson-Cook parameters in question. It should be possible to use any of the designs for optimization-based material model parameterization. The tube-based design, PC, appears to be the best choice for optimization-based material model fitting of the three considered here.

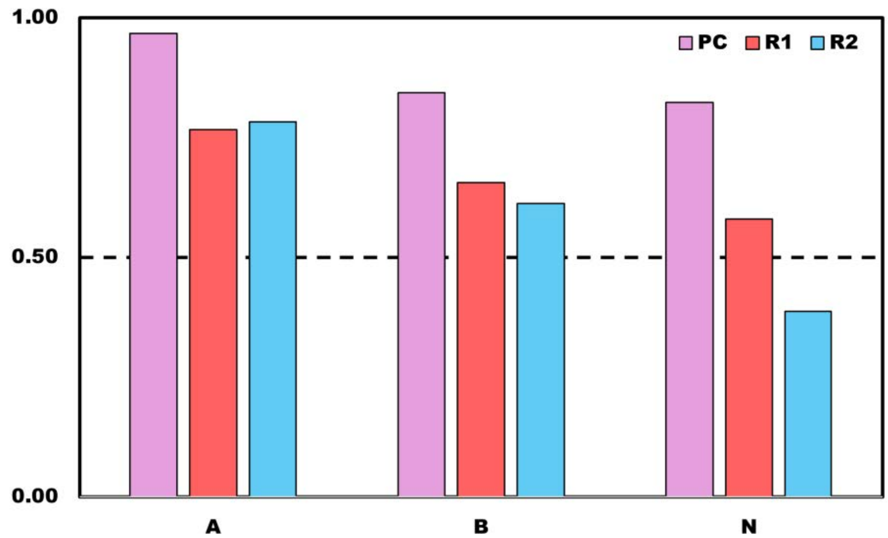

Fig. 3 Average magnitudes of the sensitivity indices for the PC, R1, and R2 for the Johnson-Cook parameters A, B, and n.

There are advantages to ring-based experimental geometries. Less sample material is required, which can be an advantage when the sample material is costly, toxic, or radioactive. It is also useful that the ring velocity data can be used to determine stress and strain directly. The R1 design appears to offer an acceptable compromise of properties which would allow it to be used for either model fitting or direct constitutive data extraction.

Conclusion

We examined three different sample tensile expansion geometries which used an RP-4 SC detonator as an energy source: a design based on a simple sample tube and two different ring-based sample designs. The three designs were evaluated by modeling using the ALEGRA hydrocode and running sensitivity analyses using DAKOTA to assess whether they would be suitable for determining the A, B, and n parameters of the Johnson-Cook constitutive model.

It appears that the tube-based design offers greater sensitivity to the Johnson-Cook constitutive parameters in question and may be a better choice for optimization-based fitting of a constitutive model. However, the ring-based designs should allow direct extraction of material constitutive model parameters more readily than the tube-based design. The first of the ring-based designs, based on using a thin disc of polymer as the driver material for the sample ring, appears to be an acceptable compromise for either model fitting or direct extraction of stress strain data.

Acknowledgments This research made use of Idaho National Laboratory's High Performance Computing systems located at the Collaborative Computing Center and supported by the Office of Nuclear Energy of the U.S. Department of Energy and the Nuclear Science User Facilities under Contract No. DE-AC07-05ID14517.

References

1. P. Johnson, B. Stein, and R. Davis, “Measurement of dynamic plastic flow properties under uniform stress,” presented at the symposium on dynamic behavior of materials, ASTM International, 1963.
2. C. Hoggatt and R. Recht, “Stress-strain data obtained at high rates using an expanding ring: Investigation indicates that dynamic symmetrical free expansion of thin rings offers a valid means for obtaining uniaxial tensile stress-strain relationships at high strain rates,” Exp. Mech., vol. 9, pp. 441–448, 1969.
3. R. Warnes, T. Duffey, R. Karpp, and A. Carden, “An improved technique for determining dynamic material properties using the expanding ring,” Shock Waves High-Strain-Rate Phenom. Met. Concepts Appl., pp. 23–36, 1981.
4. B. Aydelotte, “Analysis of the explosively driven expanding ring tension test,” presented at the Dynamic Behavior of Materials, Volume 1: Proceedings of the 2020 Annual Conference on Experimental and Applied Mechanics, Springer, 2021, pp. 73–77.
5. B. Aydelotte, P. Hibner, B. D. Brown, W. Fuger, C. Angell, and W. Jones, “Additional Study of the Explosively Driven Expanding Ring Tension Test,” in Dynamic Behavior of Materials, Volume 1, S. Mates and V. Eliasson, Eds., Cham: Springer International Publishing, 2022, pp. 83–87.
6. F. I. Niordson, “A unit for testing materials at high strain rates,” Exp. Mech., vol. 5, no. 1, pp. 29–32, Jan. 1965, doi: 10.1007/BF02320901.
7. D. Grady and D. Benson, “Fragmentation of metal rings by electromagnetic loading,” Exp. Mech., vol. 23, no. 4, pp. 393–400, Dec. 1983, doi: 10.1007/BF02330054.
8. H. Zhang and K. Ravi-Chandar, “On the dynamics of necking and fragmentation – I. Real-time and post-mortem observations in Al 6061-O,” Int. J. Fract., vol. 142, no. 3, pp. 183–217, 2006, doi: 10.1007/s10704-006-9024-7.
9. B. Aydelotte, “Fragmentation and reaction of structural energetic materials,” Goergia Institute of Technology, Atlanta, GA, 2013. [Online]. Available: http://hdl.handle.net/1853/50253
10. A. Fedorenko, Y. Sudenkov, S. Konev, and I. Sergeichev, “Exploding wire method for the characterization of dynamic tensile strength of composite materials,” Int. J. Impact Eng., vol. 180, p. 104704, Oct. 2023, doi: 10.1016/j.ijimpeng.2023.104704.
11. R. E. Winter and H. G. Prestige, “A technique for the measurement of the high strain rate ductility of metals,” J. Mater. Sci. Lett., vol. 13, no. 8, pp. 1835–1837, Jan. 1979, doi: 10.1007/BF00548753.
12. T. J. Vogler et al., “Fragmentation of Materials In Expanding Tube Experiments,” Int. J. Impact Eng., vol. 29, no. 1–10, pp. 735–746, Dec. 2003, doi: 10.1016/j.ijimpeng.2003.10.020.
13. “RP-4 SC EBW Shaped Charge.” RISI, 2020. [Online]. Available: https://www.teledynedefenseelectronics.com/energetics/Documents/RP-4SC_2020.pdf
14. T. J. Fuller et al., “ALEGRA User Manual (Code Version 8.17.5),” Sandia National Laboratories, Albuquerque, NM, Oct. 2024.
15. B. Aydelotte, C. Merriman, and W. Jones, “On Depth of Penetration Testing,” in Proceedings of the 2024 SEM Annual Conference & Exposition on Experimental and Applied Mechanics, Feb. 2024.
16. D. R. Scheffler, M. S. Burkins, and W. P. Walters, “Characterization of Jets from Exploding Bridge Wire Detonators,” Army Res. Lab Aberd. Proving Ground Md Weapons Mater. Res. Dir. ARL-TR, vol. 3518, 2005.
17. G. R. Johnson and W. H. Cook, “A constitutive model and data for metals subjected to large strains, high strain rates, and high temperatures,” in Proceedings of the 7th International Symposium on Ballistics, The Hague, Netherlands, 1983, pp. 541–547.
18. G. R. Johnson and W. H. Cook, “Fracture characteristics of three metals subjected to various strains, strain rates, temperatures and pressures,” Eng. Fract. Mech., vol. 21, no. 1, pp. 31–48, 1985, doi: doi: DOI: 10.1016/0013-7944(85)90052-9.
19. D. J. Steinberg, S. G. Cochran, and M. W. Guinan, “A constitutive model for metals applicable at high-strain rate,” J. Appl. Phys., vol. 51, no. 3, pp. 1498–1504, 1980.
20. D. J. Steinberg and C. M. Lund, “A constitutive model for strain rates from 10−4 to 106 s−1,” J. Appl. Phys., vol. 65, no. 4, p. 1528, 1989, doi: 10.1063/1.342968.
21. E. L. Lee, H. C. Hornig, and J. W. Kury, “Adiabatic Expansion Of High Explosive Detonation Products,” United States, 1968. doi: 10.2172/4783904.
22. B. M. Adams et al., “Dakota, A Multilevel Parallel Object-Oriented Framework for Design Optimization, Parameter Estimation, Uncertainty Quantification, and Sensitivity Analysis (V.6.16 User’s Manual),” Sandia National Lab. (SNL-NM), Albuquerque, NM (United States), SAND2022-6171, Nov. 2021. doi: 10.2172/1868142.